Acta Crystallographica Section D
Biological Crystallography
ISSN 0907-4449

Induced-fit motion of a lid loop involved in catalysis in alginate lyase A1-III

Bunzo Mikami,[a]*‡ Mizuho Ban,[a]§ Sachiko Suzuki,[b]¶ Hye-Jin Yoon,[a]‡‡ Osamu Miyake,[b]§§ Masayuki Yamasaki,[a]¶¶ Kohei Ogura,[b]‡‡‡ Yukie Maruyama,[b] Wataru Hashimoto[b] and Kousaku Murata[b]‡

[a]Laboratory of Applied Structural Biology, Department of Applied Life Science, Graduate School of Agriculture, Kyoto University, Gokasho, Uji, Kyoto 611-0011, Japan, and [b]Laboratory of Basic and Applied Molecular Biotechnology, Department of Food Science, Graduate School of Agriculture, Kyoto University, Gokasho, Uji, Kyoto 611-0011, Japan

‡ BM and KM contributed equally to this paper.
§ Present address: Department of Food and Nutrition, Sanyo Gakuen Junior College, 1-14-1 Hirai, Naka-ku, Okayama 703-8501, Japan.
¶ Present address: Research Institute, Gekkeikan Sake Company Ltd, 300 Katahara-cho, Fushimi-ku, Kyoto 612-8361, Japan.
‡‡ Present address: School of Chemistry, Seoul National University, Seoul 151-742, Republic of Korea.
§§ Present address: Division of Food Nutrition, Kyoto Junior College, 3370 Nishi-Kotanigaoka, Fukuchiyama, Kyoto 620-0886, Japan.
¶¶ Present address: Young Researcher Development Centre (The Hakubi Centre), Institute for Frontier Medical Sciences, Kyoto University, Sakyo-ku, Kyoto 606-8397, Japan.
‡‡‡ Present address: Department of Molecular Infectiology, Graduate School of Medicine, Chiba University, 1-8-1 Inohana, Chuo-ku, Chiba 260-0856, Japan.

Correspondence e-mail: mikami@kais.kyoto-u.ac.jp

Received 2 December 2011
Accepted 31 May 2012

PDB References: A1-III, H192 mutant, apo, 4e1y; H192 mutant, complexed with alginate tetrasaccharide, 4f10; Y246F mutant, complexed with alginate tetrasaccharide, 4f13.

The structures of two mutants (H192A and Y246F) of a mannuronate-specific alginate lyase, A1-III, from *Sphingomonas* species A1 complexed with a tetrasaccharide substrate [4-deoxy-L-*erythro*-hex-4-ene-pyranosyluronate-(mannuronate)$_2$-mannuronic acid] were determined by X-ray crystallography at around 2.2 Å resolution together with the apo form of the H192A mutant. The final models of the complex forms, which comprised two monomers (of 353 amino-acid residues each), 268–287 water molecules and two tetrasaccharide substrates, had *R* factors of around 0.17. A large conformational change occurred in the position of the lid loop (residues 64–85) in holo H192A and Y246F compared with that in apo H192A. The lid loop migrated about 14 Å from an open form to a closed form to interact with the bound tetrasaccharide and a catalytic residue. The tetrasaccharide was bound in the active cleft at subsites −3 to +1 as a substrate form in which the glycosidic linkage to be cleaved existed between subsites −1 and +1. In particular, the O$^{\eta}$ atom of Tyr68 in the closed lid loop forms a hydrogen bond to the side chain of a presumed catalytic residue, O$^{\eta}$ of Tyr246, which acts both as an acid and a base catalyst in a *syn* mechanism.

1. Introduction

The degradation of acid polysaccharides such as alginate proceeds by a lyase reaction, which produces double-bonded sugars at the nonreducing end of the product. Among the 21 families (PL-1 to PL-21) of polysaccharide lyases classified in the CAZY database (Carbohydrate Active Enzymes database; http://www.cazy.org/; Cantarel *et al.*, 2009), the structures of enzymes from 19 families have been determined (Garron & Cygler, 2010; Lombard *et al.*, 2010). In order to elucidate the mechanism by which these enzymes degrade acid polysaccharides, the structures of complexes of many lyases with ligands including the substrates and/or products of these lyases have been reported (Garron & Cygler, 2010; Lombard *et al.*, 2010; Ochiai *et al.*, 2010; Shaya *et al.*, 2010). It has been reported that the Tyr, His and Asn triad is conserved and plays an important role in the catalysis of polysaccharide lyases in the PL-5 (Yoon *et al.*, 2001), PL-7 (Ogura *et al.*, 2008; Yamasaki *et al.*, 2005; Osawa *et al.*, 2005) and PL-8 (Féthière *et al.*, 1999; Lunin *et al.*, 2004; Huang *et al.*, 2001; Li & Jedrzejas, 2001; Mello *et al.*, 2002; Nukui *et al.*, 2003; Rigden & Jedrzejas, 2003) families. There is a structural similarity between the catalytic domains of PL-5 and PL-8. In alginate lyase (PL-5; Yoon *et al.*, 2001), chondroitin AC lyase (PL-8; Féthière *et al.*, 1999; Lunin *et al.*, 2004; Huang *et al.*, 2001) and xanthan lyase

(PL-8; Maruyama *et al.*, 2005, 2007) the catalytic residue which accepts a hydrogen from C5 at the +1 sugar subsite and donates hydrogen to the glycosidic O atom to be cleaved has been reported to be a Tyr residue. In contrast, His is the proton acceptor and Tyr is the proton donor in hyaluronate lyase (PL-8; Ponnuraj & Jedrzejas, 2000; Li *et al.*, 2001; Jedrzejas *et al.*, 2002; Li & Jedrzejas, 2001; Mello *et al.*, 2002; Nukui *et al.*, 2003; Rigden & Jedrzejas, 2003; Rigden *et al.*, 2006). However, recent analysis of another PL-8 hyaluronate lyase complexed with a disaccharide suggested that Tyr is involved in proton abstraction from the substrate (Elmabrouk *et al.*, 2011).

The alginate lyase A1-III is a β-D-mannuronosyl linkage-specific (M-M-specific) enzyme that acts on alginate tetrasaccharide as the minimum substrate and produces disaccharides and trisaccharides from alginate (Murata *et al.*, 1993; Yonemoto *et al.*, 1993). The structure of an A1-III crystal at 1.78 Å resolution was reported as the first example of a family PL-5 enzyme (Yoon *et al.*, 1999). Based on the structure of A1-III complexed with a trisaccharide product, it was proposed that Tyr246 is a catalytic residue that is responsible for both the abstraction and the donation of hydrogen (Yoon *et al.*, 2001). However, the complex structure was insufficient in two respects. Firstly, the enzyme was not in an active form, having a fixed open lid-loop region (residues 64–85) caused by crystallographic interactions. Secondly, the product sugars did not bind to cover the subsites on either side of the catalytic residue (subsites −3 to −1). It is important to overcome crystallographic artifacts such as symmetry interactions and the effects of freezing in order to elucidate the conformational changes and complex formation in the enzymatic process. An accurate determination of the structure of the mutant enzyme–substrate complex without crystallographic artifacts is necessary in order to elucidate the catalytic residue (Dunlop *et al.*, 2005; Skrzypczak-Jankun *et al.*, 2006).

In this paper, we describe the crystal structures of mutant alginate lyases (H192A and Y246F) complexed with tetrasaccharide substrates at around 2.2 Å resolution. We thus determined a new crystal form of the enzyme in which the lid-loop region can move from an open to a closed form by an induced-fit motion. For the first time, we were able to determine the structure of a sugar bound at subsite +1 in the closed lid-loop form. We used crystals enclosed in capillaries in order to avoid the effects of freezing.

2. Materials and methods

2.1. Preparation of mutant enzymes

A1-III mutants with mutations of the amino-acid residues in the active site (Y246F, H192A, G60A, R67A, Y68F and Y80F) were prepared by site-directed mutagenesis with plasmid pET3a-A1-III (Yoon *et al.*, 2000) as a template using the QuikChange Site-Directed Mutagenesis kit (Stratagene, La Jolla, California, USA) according to the manufacturer's instructions. The mutated genes were amplified by PCR. *Escherichia coli* strain BL21(DE3)pLysS (Novagen Inc., Madison, Wisconsin, USA) was used as a host for expression of the mutated genes. The mutations were confirmed by analysis of the nucleotide sequences of the mutated genes. The transformants of *E. coli* BL21(DE3)pLysS with the plasmids containing each mutated gene produced large volumes of mutant enzymes in soluble form. Purification and activity assays of the mutant enzymes were performed as described previously (Yoon *et al.*, 2000).

2.2. Crystallization and structure analysis

Using numerous crystallization screens, we obtained several crystal forms of the H192A and Y246F mutants in space groups including that of the original A1-III structure (*C*2; Yoon *et al.*, 1999, 2001), $P2_1$ and $P2_12_12_1$. Among these crystal forms, only the $P2_12_12_1$ crystal had a mobile lid-loop region without symmetry-packing interactions. The $P2_12_12_1$ crystals of these mutants were obtained by the hanging-drop vapour-diffusion method against 24%(*w*/*v*) PEG 4000, 0.3 *M* ammonium acetate, 0.1 *M* sodium citrate pH 5.5 at 293 K with a protein concentration of around 10 mg ml^{-1}. Prismatic crystals appeared in a month. Holoenzyme crystals were obtained by soaking these crystals with 12.5–50 m*M* alginate tetrasaccharide at 293 K for 30 min. In order to avoid the release of substrate from the enzyme during freezing, data collection was carried out by the capillary method at 293 K. The crystals and a drop of the mother liquor were placed in a glass capillary sealed with dental wax at both ends. Diffraction data were collected from apo and holo H192A crystals on an in-house multi-wire detector (Hi-Star; Bruker, Karlsruhe, Germany) with Cu $K\alpha$ radiation generated by a rotating-anode generator (M18XHF; MacScience, Tokyo, Japan) at 293 K. The raw data images were processed using the *SADIE* and *SAINT* software packages (Bruker). The diffraction data of holo Y246F crystals were collected on the BL38B1 beamline of SPring-8 by the capillary method at 298 K using a CCD detector (Quantum 4; ADSC, Poway, California, USA) at a wavelength of 1.0 Å. The collected images were processed with the *HKL*-2000 package (Otwinowski & Minor, 1997).

The structures of the H192A and Y246F mutants were determined by molecular replacement with the *CNS_SOLVE* package (Brünger *et al.*, 1998) using wild-type A1-III (PDB entry 1qaz; Yoon *et al.*, 1999) as a search model. The final refinement of the structures was carried out by *PHENIX* (Adams *et al.*, 2010) using noncrystallographic symmetry restraints. The models were rebuilt using *TURBO-FRODO* (CNRS, France) and *Coot* (Emsley *et al.*, 2010). The stereochemical quality of the final models was assessed using *PROCHECK* (Laskowski *et al.*, 1993) and *WHATCHECK* (Hooft *et al.*, 1996). The puckering parameters (Cremer & Pople, 1975) of the bound alginate tetrasaccharides were calculated using the *PLATON* package (Spek, 2003). The subsite numbers of the bound tetrasaccharides were designated as −3, −2, −1 and +1 from the reducing end based on the rule of Davies *et al.* (1997). The accessible surface area was calculated by the program *NACCESS* (Hubbard & Thornton, 1993). The *CCP*4 package (Winn *et al.*, 2011) was used for the

Table 1
Kinetic parameters of the mutant enzymes.

Enzyme	K_m (mg ml^{-1})	V_{max} ($\Delta A_{235\ nm}$ min^{-1} mg^{-1})	V_{max} (%)	Relative V_{max}/K_m (%)
Wild type	0.041	72.7	100	100
H192A	0.027	0.0030	0.0033	0.0050
Y246F	0.079	0.0024	0.011	0.0057
G60A	0.056	21.8	80.0	58.6
M62P, intact	0.050	32.0	44.0	42.0
M62P, nicked	0.029	0.011	0.015	0.020
R67A	0.169	22.5	31.0	7.5
Y68F	0.177	16.0	22.0	5.1
Y80F	0.038	35.6	49.0	52.9

manipulation of data and coordinates. The figures were drawn using *PyMOL* (v.1.19; Schrödinger LLC).

2.3. Preparation of alginate tetrasaccharide

Alginate tetrasaccharide was prepared from a digest of alginate with A1-III by gel filtration as described previously (Yoon *et al.*, 2001).

2.4. Amino-acid sequencing

The N-terminal protein sequence of mutant alginate lyase A1-III (M62P) was analyzed by Edman degradation in a pulsed liquid-phase protein sequencer (Procise 492; Applied Biosystems) after blotting the SDS gel onto a polyvinylidene membrane.

2.5. Alignment of amino-acid sequences

The multiple alignment of the amino-acid sequences of mannuronate-specific alginate lyases from *Pseudomonas syringae* (Preston *et al.*, 2000), *P. fluorescens* (Gimmestad *et al.*, 2003), *P. aeruginosa* (Boyd *et al.*, 1993), *Cobetia marina* (Swiss-Prot Q9ZNB7) and *Azotobacter chroococcum* (Peciña *et al.*, 1999) was performed using *ClustalW* (Thompson *et al.*, 1994).

3. Results and discussion

3.1. Mutation of residues in the active site and lid loop of A1-III

Both the mutant of the assumed catalytic residue, Y246F, and that of the adjacent residue, H192A, showed large decreases in V_{max} values of the order of 10^{-5} compared with the wild-type enzyme (Table 1). The mutants of the residues on the lid loop (residues 57–90), G60A, M62P, R67A, Y68F and Y80F, showed V_{max} values that were 22–80% lower than that of the wild-type enzyme. After Y246F and H192A, Y68F showed the largest effect on the activity, decreasing the V_{max}/K_m value to 5.1% of the value for the wild-type enzyme. Two components of M62P, intact M62P and nicked M62P, were found during purification of the mutant enzyme. Analysis of the N-terminal amino acids of the fragments of the nicked form indicated two sequences derived from the N-terminus (^{1}MHPFD . . .) and from the cleaved site (^{67}RYLSE . . .), suggesting that amino acids in the vicinity of Arg66 are deleted in the nicked form owing to proteolysis during purification. The large decrease in the activity of the nicked M62P (of the order of 10^{-4}) suggests the importance of the lid loop for enzymatic activity.

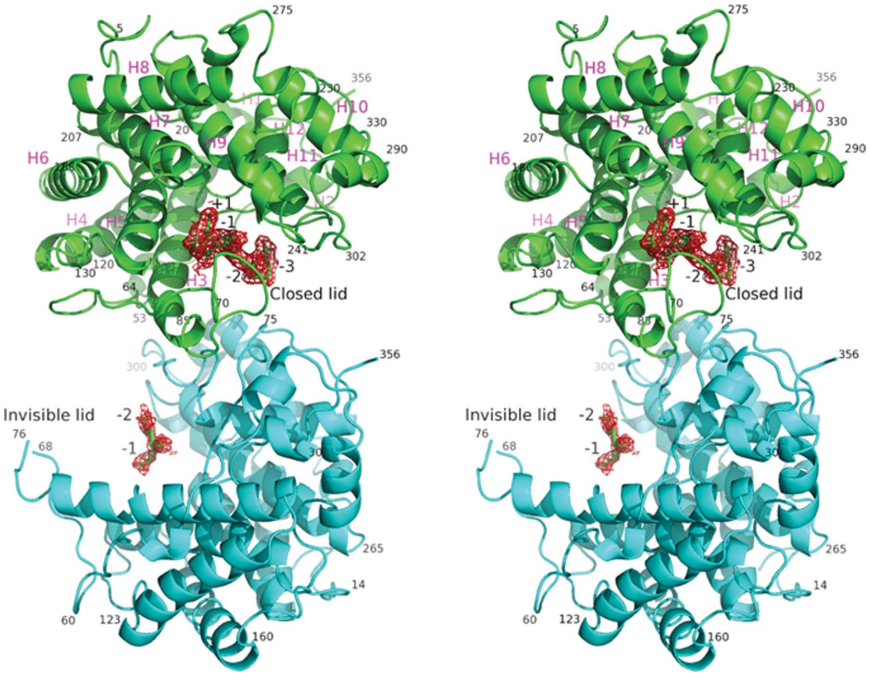

Figure 1
Overall structure of the asymmetric unit of holo Y246F (stereoview). The $|F_o| - |F_c|$ density map countered at 3.0σ around the bound tetrasaccharide is shown as a red mesh. Molecules *A* and *B* are coloured green and cyan, respectively. The open and closed lid loops in molecule *B* are shown in cyan and blue, respectively. The sequence number and subsite number of the bound sugar are labelled. The secondary-structure elements (H1–H12) according to Yoon *et al.* (1999) are shown in magenta.

3.2. Quality of the final models

In the preliminary crystallization screening several crystal forms were obtained, but most of them had a fixed open loop owing to symmetry interactions in the crystal packing. Even in the present $P2_12_12_1$ crystals the open lid loop in one of the two molecules in the asymmetric unit makes weak interactions with an adjacent symmetry molecule. The other problem arose owing to crystal cooling, which resulted in dissociation of the substrate from the molecule, as described previously (Yoon *et al.*, 2001). In the present work, therefore, we collected crystallographic data by the capillary method without cooling. The refinement of the apo H192A, holo H192A and holo Y246F structures was carried out

Table 2
Data-collection and refinement statistics for mutant A1-III.

Values in parentheses are for the highest resolution shell.

	Apo H192A	H192A–tetrasaccharide	Y246F–tetrasaccharide
Substrate (m*M*)	0	50	12.5
Diffraction data			
X-ray source	In-house	In-house	BL38B1, SPring-8
Wavelength (Å)	1.54	1.54	1.00
Detector	Hi-Star multiwire	Hi-Star multiwire	Quantum-4 CCD
Space group	$P2_12_12_1$	$P2_12_12_1$	$P2_12_12_1$
Unit-cell parameters (Å)	a = 65.44, b = 76.99, c = 143.52	a = 65.43, b = 77.60, c = 145.75	a = 65.57, b = 77.56, c = 145.68
Resolution limits (Å)	40.6–2.10 (2.22–2.10)	41.2–2.20 (2.28–2.20)	48.7–2.20 (2.24–2.20)
Measured reflections	186118 (14476)	213009 (10552)	196763 (9785)
$\langle I/\sigma(I)\rangle$	12.1 (2.6)	13.2 (2.8)	16.7 (3.0)
Unique reflections	41806 (6213)	38230 (3686)	36529 (3116)
Completeness (%)	97.0 (93.2)	99.4 (97.5)	96.2 (95.9)
R_{sym} or R_{merge} (%)	6.2 (29.8)	8.9 (36.7)	9.8 (48.4)
Wilson B (Å^2)	20.8	17.2	25.7
Refinement			
Resolution range (Å)	40.6–2.10 (2.16–2.10)	41.2–2.20 (2.26–2.20)	48.7–2.21 (2.27–2.21)
Reflections used	41806 (2601)	38167 (2630)	36472 (2603)
Completeness (%)	97.0 (92.4)	99.5 (97.2)	95.9 (91.0)
Residues/waters	706/287	693/286	699/270
Disordered residues	14	11	12
Tetrasaccharide	—	ΔM-G-M-M/G-M	ΔM-M-M-M/M-M
Sugar-occupied sites	—	+1 to −3/−1 to −2	+1 to −3/−1 to −2
Lid-loop position (*A*/*B*)	Open/open	Closed/not visible	Closed/not visible
Average B factor (Å^2)	29.5	25.2	30.8
Bond-length r.m.s.d. (Å)	0.012	0.013	0.010
Bond-angle r.m.s.d. (°)	1.33	1.37	1.31
R factor (%)	16.3 (28.7)	19.4 (31.8)	17.7 (24.8)
R_{free} (%)	20.6 (36.7)	23.9 (34.8)	21.4 (32.7)

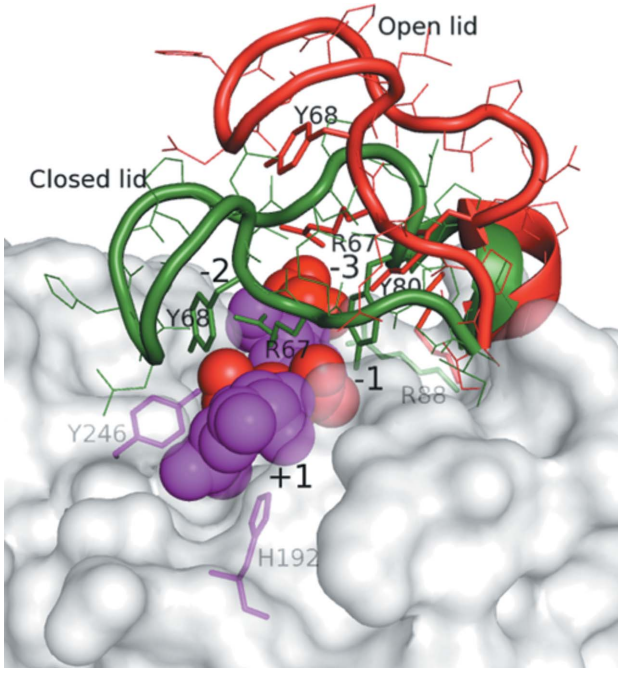

Figure 2
Lid-loop motion in the active site of A1-III. The open (red) and closed (green) lid loops are shown together with the bound tetrasaccharide (circles) on the molecular surface after superposition of apo and holo H192A. The sugar residues at subsites +1 to −3 are shown in magenta and red, alternately.

by *PHENIX*, as shown in Table 2. The final holo-form models contained 2 × 353 amino-acid residues, 270–286 water molecules and two alginate tetrasaccharides (Fig. 1). There are 11–14 disordered residues in the structures. The invisible parts of molecule *B* in the holo-form models around residues 66–77 and two sugars were deleted from the final model. The *R* factors (R_{free}) for the data to 2.1–2.2 Å resolution were 0.163 (0.206), 0.194 (0.239) and 0.177 (0.214) for apo H192A, holo H192A and holo Y246F, respectively. In the Ramachandran plots (Ramachandran & Sasisekharan, 1968; Laskowski *et al.*, 1993), 98.8, 99.7 and 99.7% of nonglycine residues were in the most favoured and additionally allowed regions, respectively. The absolute coordinate errors estimated from Luzatti plots (Luzzati, 1952) were 0.20–0.23 Å, respectively. The r.m.s. distances of the two molecules in an asymmetric unit were 0.31, 0.35 and 0.31 Å for 343, 340 and 333 C^{α} atoms for apo H192A, holo H192A and holo Y246F, respectively. In the structures of holo H192A and Y246F one molecule (molecule *A*) has a closed lid loop, while the other (molecule *B*) has an invisible lid loop that may be alternately opened and closed. Because the electron-density map of the lid loop and the bound sugar in molecule *B* is poor owing to low occupancy and high *B* factors, we used the structures of molecule *A* of holo H192A and Y246F in the following analysis of enzyme–substrate interactions (Fig. 1).

3.3. Overall structure

A large conformational change of the lid loop (residues 64–85) was found between the structures of the apo (H192A) and the holo forms (H192A and Y246F), as shown in Figs. 1 and 2. The secondary-structure elements (H1–H12) were defined as described in Yoon *et al.* (1999). The open lid loop that protruded into the solvent moved to the closed form by bending at the middle of L2 (the loop connecting H2 and H3; residues 44–79) and part of H3 (residues 80–105), with the result that the active-site cleft was covered (Figs. 1 and 2). The r.m.s. distance between apo and holo H192A was 0.62 Å for 353 C^{α} atoms of molecule *A*, while that between holo H192A and holo F246Y was 0.17 Å, suggesting that the difference was caused by the conformational change of the lid loop. Fig. 3(*a*) shows *B*-factor plots for apo and holo H192A (molecule *A*) along the sequence together with the r.m.s. distance between the two molecules. The average *B* factor of the lid-loop region (residues 64–85) is high in the apoenzyme (47.4 Å^2), but becomes lower in holo H192A (23.1 Å^2) in accord with the

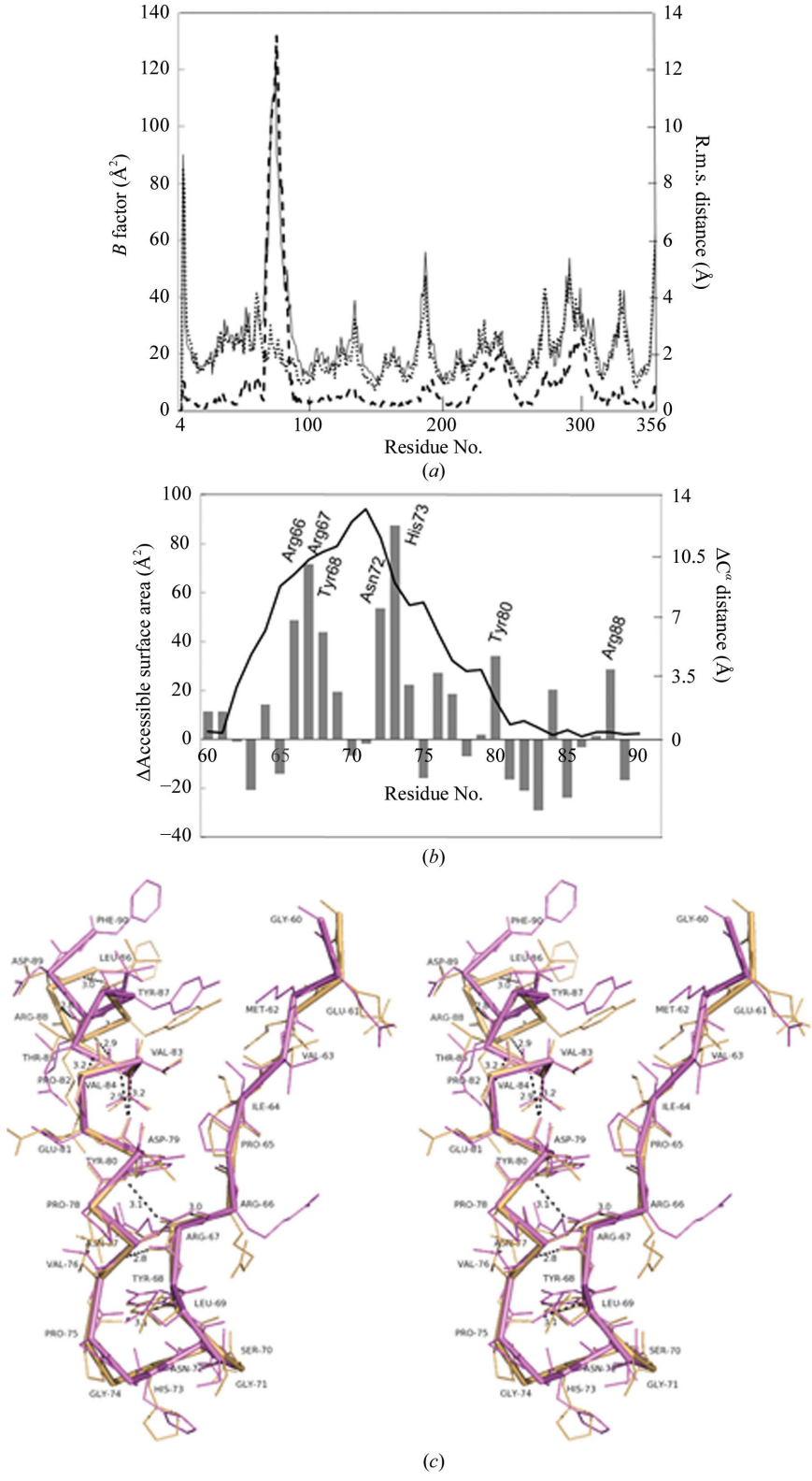

Figure 3
(*a*) The average *B* factors and the r.m.s. distance between apo and holo H192A along the amino-acid sequence. The average *B* factors of apo and holo H192A are indicated by straight and dotted lines, respectively. The r.m.s. distance of C^{α} atoms is indicated by a thick dashed line. The lid-loop region (residues 64–85) has the highest *B* factor in the apo form and the largest r.m.s. distance. (*b*) The r.m.s. distance and the change in accessible surface area of residues on the lid loop of H192A are represented by a line and by bars, respectively. (*c*) Superposition of the open (magenta) and closed (yellow) lid loops of H192A after superposition of 22 C^{α} atoms in the lid loop (residues 64–85) (stereoview).

peak in the r.m.s. distance plot. The maximum movement increases in residues 73–75, reaching 13.4 Å between C^{α} atoms at Gly74.

The two molecules (molecules *A* and *B*) in the asymmetric unit behaved differently in the holo structures. Molecule *A* has a completely closed lid loop, but molecule *B* has invisible lid loops (Fig. 1). The two molecules have different crystal packings. The open lid loop of molecule *B* in apo H192A makes interactions with the adjacent molecule *B* including three hydrogen bonds (Asp79 $O^{\delta2}\cdots$#Arg276 $N^{\eta1}$, 2.8 Å; Pro78 O $\cdots$Wat$\cdots$#Glu229 N, 2.7 and 2.9 Å) and two C—C contacts (Pro82 $C^{\gamma}\cdots$#Glu229 C^{β}, 3.6 Å; Pro78 $C^{\beta}\cdots$#Asn228 C^{α}, 4.0 Å). Thus, the lid loop of molecule *B* is fixed in an open position. In contrast, the open lid loops of molecule *A* in holo H192A and holo Y246F make weak interactions with molecule *B* in the same asymmetric unit, including a few van der Waals contacts with C—C distances less than 4.4 Å (Pro75*A*$\cdots$Asp37*B*, Pro78*A* $\cdots$Ala41*B*, Pro78*A*$\cdots$Val336*B*, Pro82*A*$\cdots$ Val336*B*, Thr85*A*$\cdots$Lys309*B* and Glu81*A* $\cdots$Thr335*B*). The binding of tetrasaccharide results in complete and partial lid-loop closure in molecules *A* and *B*, respectively, in the capillary crystals. However, crystal cooling resulted in the complete opening of both lid loops and the release of the bound tetrasaccharide, possibly owing to shrinkage of the crystal lattice and the resulting increase in the above interactions, as described for other proteins (Dunlop *et al.*, 2005; Skrzypczak-Jankun *et al.*, 2006). In addition to cell shrinkage, cooling may change the pH of the solvent in the crystal. Moreover, cryoprotectants such as glycerol and MPD are potent inhibitors of sugar-related enzymes such as alginate lyase (Tsitsanou *et al.*, 1999).

3.4. Lid-loop motion

Superposition of the open and closed lid loops suggests that the conformational change results in near-rigid-body motion (Fig. 3*c*). The r.m.s. deviation of the 22 C^{α} pairs (residues 64–85) of the open and closed lid loops is only 0.46 Å. At the N-terminus of the mobile lid loop, Ile64 makes the hinge by changing its main-chain dihedral angles from $(\varphi, \psi) = (-98^{\circ}, 116^{\circ})$ in the open form to $(-137^{\circ}, 126^{\circ})$ and $(-132^{\circ}, 128^{\circ})$ in the H192A and Y246F closed forms,

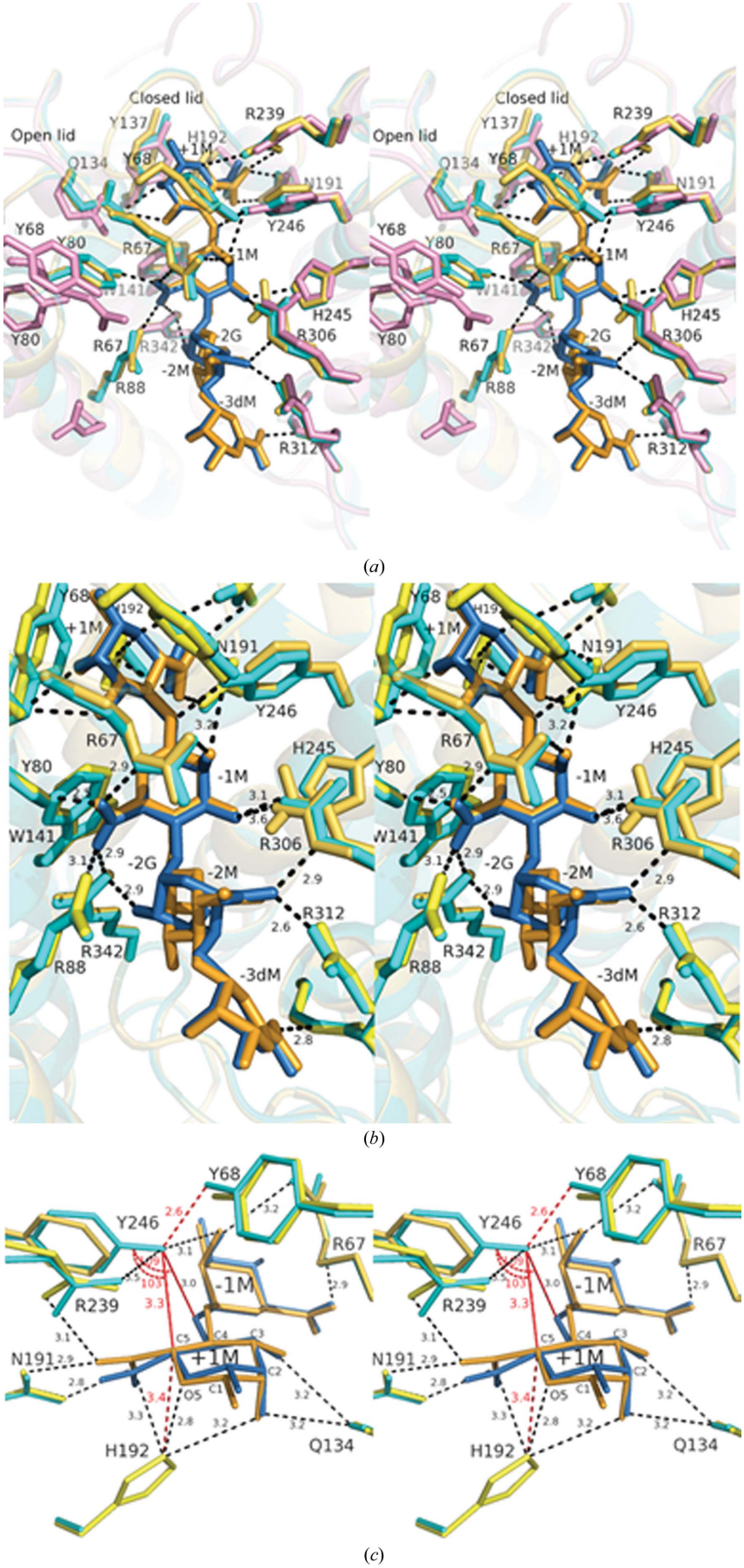

respectively. In contrast, at the C-terminus of the lid loop the movement ended gradually in the middle of the H3 helix through small changes in dihedral angles from residues 82 to 85, resulting in an approximately 19° bend of H3 (Fig. 2).

The open–closed movement of the lid loop decreases the accessible surface area of 582 Å^2 by covering the active-site cleft. In particular, the side chains of Arg66, Arg67, Tyr68, Asn72, His73, Tyr80 and Arg88 are buried in the closed lid loop (Fig. 3*b*). Most of these residues are important for interaction with the substrate. The side chains of Tyr68 and Asn72 make three nascent hydrogen bonds to residues in the cleft of holo H192A (Tyr68 O$^{\eta}\cdots$Tyr246 O$^{\eta}$, 2.6 Å; Asn72 O$\cdots$Arg239 N$^{\eta 2}$, 2.7 Å; Asn72 O$\cdots$Arg239 N$^{\varepsilon}$, 3.3 Å). Because the closed lid loop completely covers the active-site cleft, it should be open during the release of the product and the incorporation of the next substrate (Fig. 2). The motion of the lid loop is classified as a fragment motion of the hinge mechanism (Gerstein & Krebs, 1998). The fragment region of 22 residues including part of H3 is larger than the usual ω-loop with an open and closed motion, as represented by triose phosphate isomerase (Noble *et al.*, 1993).

3.5. Structure of bound alginate tetrasaccharide

From the density of the bound tetrasaccharide, it is suggested that the H192A and Y246F mutants bind different alginate tetrasaccharides in their active sites (Figs. 4*a* and 4*b*). In the Y246F holo form, the four sugar residues were identified as β-mannuronate (M) at subsites between +1 and −2 and a double-bonded sugar (ΔM) at subsite −3, while the β-mannuronate at subsite −2 was replaced by an α-guluronate (G) in the case of the H192A holo form.

Figure 4
Interaction of the tetrasaccharide with protein residues in H192A and Y246F (stereoview). (*a*) The structures of apo H192A, holo H192A and holo Y246F are shown in pink, cyan and yellow, respectively. Estimated hydrogen bonds are shown as broken lines. (*b*) Close-up view around the −1 and −2 sites after superposition of H192A (cyan) and Y246F (yellow). (*c*) Close-up view around the +1 sites after superposition of H192A (cyan) and Y246F (yellow). The Tyr246 O$^{\eta}\cdots$C5, His192 N$^{\varepsilon 2}\cdots$C5 and Tyr246 O$^{\eta}\cdots$Tyr68 O$^{\eta}$ distances are shown in red.

Because the alginate tetrasaccharide used in the present experiment is a mixture mainly consisting of mannuronate, the substrate specificity of these two mutants is likely to be slightly different. Table 3 shows the sugar-puckering parameters (Cremer & Pople, 1975) and *B* factors of the bound sugar residues. The outer sugars (subsites +1 and −3) have higher *B* factors than the inner sugars (subsites −1 and −2). The inner sugars (subsites −1 and −2) have a chair conformation and the double-bonded sugars (ΔM) at the nonreducing ends (subsite −3) have an envelope conformation. It is interesting that the sugars at subsite +1 have a conformation that is slightly distorted from the complete chair form, although their precise conformation should be determined in a higher resolution experiment. The sugar dihedral angles (φ and ψ) of both complexes between subsites +1 and −1, subsites −1 and −2, and subsites −2 and −3 as shown in Table 3 are in the stable region for mannuronate disaccharide (Braccini *et al.*, 1999).

Table 3
B factors and sugar-pucker parameters for bound tetrasaccharide.

The dihedral angles are defined as φ, O5—C1—O4′—C4′, and ψ, C1—O4′—C4′—C5′.

Site	Residue	Mutant	*B* (Å^2)	φ (°)	θ (°)	*Q* (Å)	Form	Anomer	φ (°)	ψ (°)
+1	M	H192A	48.0	95.4	15.7	0.551	Near $^4C_1$	β		
+1	M	Y246F	39.3	91.6	15.9	0.553	Near $^4C_1$	β		
		H192A							−19.0	−175
		Y246F							−62.3	−139
−1	M	H192A	19.1	117	4.27	0.593	$^4C_1$	β		
−1	M	Y246F	27.5	132	6.64	0.583	$^4C_1$	β		
		H192A							−75.3	−91.0
		Y246F							−64.8	−103
−2	G	H192A	29.2	336	177	0.600	$^1C_4$	α		
−2	M	Y246F	33.9	177	4.59	0.596	$^4C_1$	β		
		H192A							−50.4	−117
		Y246F							−59.6	−104
−3	ΔM	H192A	45.5	118	54.4	0.505	^2E	β		
−3	ΔM	Y246F	41.5	122	55.0	0.491	^2E	β		

Table 4
Interactions between bound sugar atoms and protein atoms (molecule *A*).

The residues in the lid loop are shown in bold.

		Hydrogen-bond distance (Å)		
Sugar atom	Protein atom	H192A	Y246F	C···C contacts less than 4.4 Å
Site −3, ΔM				
O61	Gly313 N	2.8	2.9	Arg312
Site −2, G				
O2	Arg342 N$^{\eta1}$	2.9		Arg306
O3···Wat1···	Asp314 O$^{\delta2}$	2.8, 2.6		
O61	Arg312 N$^{\eta2}$	2.6		
O61	Arg306 N$^{\eta2}$	2.9		
Site −2, M				
O2···Wat1···	Asp314 O$^{\delta2}$		3.0, 2.6	Arg306, Arg88
O62	Arg312 N$^{\eta2}$		2.7	
O62	Arg306 N$^{\eta1}$		2.7	
Site −1, M				
O2	**Arg67** N$^{\eta1}$	3.2	3.3	**Arg67**, **Tyr80**, Trp141
O2	Tyr246 O$^{\eta}$	3.2		Tyr246, Tyr249
O3	His245 N$^{\varepsilon2}$	3.1	3.2	
O3	Arg306 N$^{\eta2}$	3.6	3.4	
O3···Wat1···	Asp314 O$^{\delta2}$	2.6, 2.6	2.6, 2.6	
O61	Arg88 N$^{\eta2}$	3.1	3.2	
O61	Arg342 N$^{\eta1}$	2.9	2.9	
O61···Wat2···	Gln138 O$^{\varepsilon1}$	2.9, 2.8	2.8, 3.0	
O61···Wat2···	Arg342 N$^{\eta2}$	2.9, 2.7	2.8, 2.8	
O62	**Tyr80** O$^{\eta}$	2.5	2.4	
O62	**Arg67** N$^{\varepsilon}$	2.9	3.1	
O62	Arg88 N$^{\eta2}$	3.3	3.2	
Site +1 M				
O2	His192 N$^{\varepsilon2}$	—	3.2	**Arg67**, **Tyr68**, Gln134
O2	Gln134 O$^{\varepsilon1}$	3.2	3.3	
O3	Gln134 N$^{\varepsilon2}$	3.2	3.2	Tyr137, Trp141, Asn191
O4	Tyr246 O$^{\eta}$	3.0	—	Tyr246
O5	His192 N$^{\varepsilon2}$	—	2.9	
O61	Asn191 O$^{\delta1}$	3.1	2.9	
O61	Arg239 N$^{\eta1}$	2.9	3.1	
O62	Asn191 N$^{\delta2}$	3.1	2.8	

3.6. Interactions between the closed lid loop and the substrate

The present experiment clearly shows that the two mutants bind tetrasaccharide in a productive manner by covering the catalytic site of the enzyme. The positions of the three sugar residues (subsites −1 to −3) are almost the same as those in the previous complex of the wild-type enzyme with a trisaccharide product in an open-lid conformation (Yoon *et al.*, 2001). Several residues on the closed lid loop interact with the sugar at subsite −1 and also with the sugar at subsite +1, as shown in Fig. 4 and Table 4. The side chains of Arg67, Tyr80 and Arg88 make four hydrogen bonds to mannuronate at subsite −1 (Table 4). These residues are buried in the closed lid loop (Fig. 3*b*). Among these residues, the side chain of Arg88 located near the C-terminus of the lid loop moves about 5.5 Å to interact with the sugar at subsite −1, independently of the lid-loop motion (Fig. 3*a*). The interactions of the bound sugars and protein residues are almost the same in H192A and Y246F, except at subsite −2 (Fig. 3*b*). Both mannuronate (Y246F) and guluronate (H192A) can bind at subsite −2 by forming three and four hydrogen bonds, respectively, each including one water-mediated hydrogen bond (Table 4).

3.7. Catalytic mechanism of A1-III

Comparison of the structures of holo H192A and holo Y246F provided an important clue to the mechanism of this

enzyme. In the H192A holo structure, Tyr246 O^{η} makes two hydrogen bonds to O4 of mannuronate at subsite +1 and O2 of mannuronate at subsite −1. The distance between Tyr246 O^{η} and C5 of mannuronate at subsite +1 is only 3.3 Å, suggesting that Tyr246 can extract a hydrogen from the C5 atom (Fig. 5). In contrast, the side chain of His192 in holo Y246F is situated at the other side of Tyr246 and makes two hydrogen bonds to O2 and O5 of mannuronate at subsite +1, with the distance between His192 $N^{\varepsilon 2}$ and C5 of mannuronate at subsite +1 being 3.4 Å (Figs. 1 and 3*c*). The mannuronate at subsite +1 in both holo structures has a near-chair form (Table 3), with the H atom of C5 facing towards the side chain of Tyr246. It is suggested from the distance between Tyr246 O^{η} and O4 of mannuronate at subsite +1 (2.9 Å) that Tyr246 O^{η} can also donate a hydrogen to O4 of the glycoside bond to be cleaved. The $C^{\zeta}\cdots O^{\eta}\cdots$C5 and $C^{\zeta}\cdots O^{\eta}\cdots$O4 angles are 103° and 109°, respectively (Fig. 3*c*), suggesting that the reaction coordinates are almost the same for abstraction and donation. Thus, in this lyase reaction without conformational change of the side chain, the side chain of Tyr246 is responsible for both the abstraction and donation of hydrogen simultaneously, as shown in the schematic view in Fig. 5. Several positively charged side chains, Arg239 (3.5 Å from Tyr246 O^{η}), Arg67 (4.8 Å), Arg306 (6.1 Å), His245 (5.4 Å) and His192 (6.4 Å), surrounding Tyr246 O^{η} may reduce the pK_a of Tyr246 and facilitate the abstraction and donation of H atoms. For abstraction of the H atom to occur, the sugar ring must be distorted with a coplanar C3—C4—C5—O5 configuration similar to the product double-bonded sugar. The slightly distorted sugar rings of subsite +1 in both mutant structures suggest that some additional residues other than Tyr246 and His192 may be responsible for distortion of the sugar ring at subsite +1. These residues are estimated to be Asn191 and Arg239 based on their interaction with mannuronate at subsite +1. The side-chain atoms of Asn191 and Arg239 are near O6 and O5 of mannuronate at subsite +1, respectively (Fig. 3*c* and Table 4). These side chains collaborate with His192 to distort the sugar ring and assist in the catalysis conducted by the side chain of Tyr246. These residues have also been shown to be important in chondroitin AC lyase (PL-8; Lunin *et al.*, 2004; Huang *et al.*, 2001), hyaluronate lyase (Li & Jedrzejas, 2001; Mello *et al.*, 2002; Nukui *et al.*, 2003; Rigden & Jedrzejas, 2003) and xanthan lyase (Maruyama *et al.*, 2005, 2007).

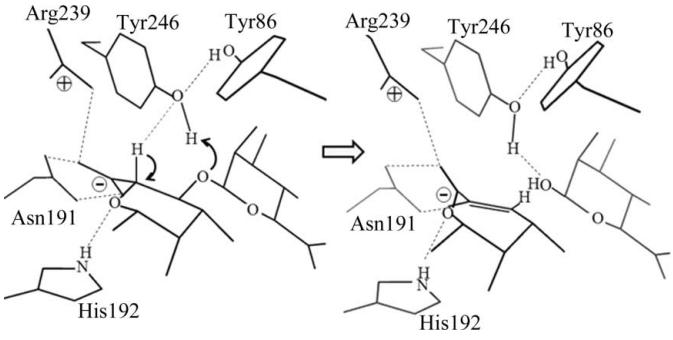

Figure 5
Schematic representation of the catalytic mechanism of alginate lyase A1-III. The side chain of Tyr246 is responsible for simultaneous abstraction and donation of hydrogen without side-chain conformational change. The side chain of Tyr68 in the closed lid loop forms a hydrogen bond to the side chain of Tyr246 that accelerates proton transfer.

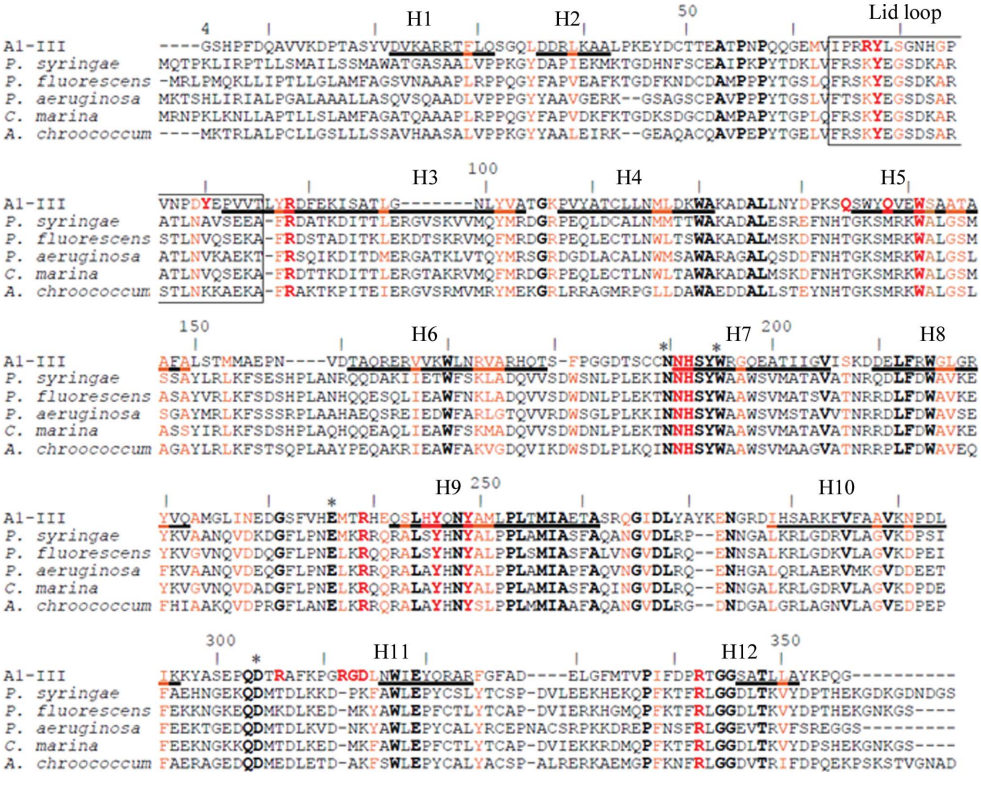

Figure 6
Multiple sequence alignment of mannuronate-specific alginate lyases belonging to the PL-5 family. The position of the lid loop in A1-III is boxed. Identical residues are shown in bold. The A1-III residues involved in interaction with the substrate are labelled in red. Conserved residues are labelled in orange. The helices in A1-III are underlined. The conserved amino-acid residues in the active site of A1-III that are not involved in direct interaction with substrate are marked by asterisks.

The present experiment also showed the important role of the lid loop in the activation of Tyr246. The side chain of Tyr68 in the closed lid loop makes a hydrogen bond to the side chain of Tyr246 (Tyr68 $O^{\eta}\cdots$Tyr246 O^{η}, 2.6 Å) and is near the positively charged side chain of Arg67 (Tyr68 $O^{\eta}\cdots$Arg67 $N^{\eta 1}$, 3.3 Å) (Figs. 3*c* and 4). We speculate that when Tyr68 O^{η} donates its hydrogen to Tyr246 O^{η} to make the hydrogen bond, the pK_a value of Tyr246 decreases by stabilizing

the deprotonated form, thereby accelerating proton transfer. The results for the mutation of Tyr68 to Phe68 (Table 1) showed that the side chain of Tyr68 accelerates catalysis by about 20-fold, which is consistent with this hypothesis.

3.8. Sequence comparison of PL-5 alginate lyase

Fig. 6 shows a sequence alignment of mannuronate-specific lyases in PL-5. The sequence around Tyr246 and His192 of A1-III is strongly conserved in the six sequences from various microorganisms. Although the sequence similarity in the lid loop region is not as high as the similarity in the regions of Tyr246 and His192, Tyr68 and Arg88 are well conserved. The position of Arg67 in A1-III is conserved as an Arg or a Lys residue. This conservative replacement is also found for Asn72 (Asp), Gly74 (Ala), Asp79 (Asn) and Tyr87 (Phe). These results suggest that the mobile lid loop of A1-III is functional throughout the family of PL-5 mannuronate-specific alginate lyases.

4. Conclusion

The crystal structures of alginate lyase mutants (Y246F and H192A) complexed with alginate tetrasaccharide have been explored in this study. The lid loop (residues 64–85) of alginate lyase A1-III can move with a maximum distance of 13.4 Å from the open form (apoenzyme) to the closed form (holoenzyme) in the orthorhombic crystal system. The conformational change of this loop is a near-rigid-body motion with hinges around residues 64 and 82–85. The conformational change is larger than the usual loop motion of the ω loop, as the lid loop contains a longer loop and part of the α-helix (H3) region. The closed lid loop interacts with the bound tetrasaccharide and a catalytic residue. In particular, Tyr68 in the closed lid loop was expected to activate a presumed catalytic residue, Tyr246, by forming a hydrogen bond. From alignment of primary structures of PL-5 mannuronate-specific alginate lyases, the lid loop seems to be conserved in this family of enzymes. The tetrasaccharide formed a bond in the active cleft at subsites −3 to +1 as a substrate form in which the glycosidic linkage to be cleaved is present between subsites −1 and +1. Based on the configuration of Tyr246 towards the substrate sugar, it is concluded that the side chain of Tyr246 acts as both an acid and a base catalyst in a *syn* mechanism.

Diffraction data for Y246F were collected at the BL-38B1 station of SPring-8 (Hyogo, Japan) with the approval of JASRI (Proposal No. C99A24XU-003N). Computation time was provided by the Supercomputer Laboratory, Institute for Chemical Research, Kyoto University, Japan. This work was supported in part by a Grant-in-Aid for Scientific Research from the Ministry of Education, Science, Sports and Culture of Japan and by Research Fellowships from the Japan Society for the Target Protein Project. Part of this work was also supported by the Program of Basic Research Activities for Innovative Biosciences (PROBRAIN) of Japan.

References

Adams, P. D. *et al.* (2010). *Acta Cryst.* D**66**, 213–221.
Boyd, A., Ghosh, M., May, T. B., Shinabarger, D., Keogh, R. & Chakrabarty, A. M. (1993). *Gene*, **131**, 1–8.
Braccini, I., Grasso, R. P. & Pérez, S. (1999). *Carbohydr. Res.* **317**, 119–130.
Brünger, A. T., Adams, P. D., Clore, G. M., DeLano, W. L., Gros, P., Grosse-Kunstleve, R. W., Jiang, J.-S., Kuszewski, J., Nilges, M., Pannu, N. S., Read, R. J., Rice, L. M., Simonson, T. & Warren, G. L. (1998). *Acta Cryst.* D**54**, 905–921.
Cantarel, B. L., Coutinho, P. M., Rancurel, C., Bernard, T., Lombard, V. & Henrissat, B. (2009). *Nucleic Acids Res.* **37**, D233–D238.
Cremer, D. & Pople, J. A. (1975). *J. Am. Chem. Soc.* **97**, 1354–1358.
Davies, G. J., Wilson, K. S. & Henrissat, B. (1997). *Biochem. J.* **321**, 557–559.
Dunlop, K. V., Irvin, R. T. & Hazes, B. (2005). *Acta Cryst.* D**61**, 80–87.
Elmabrouk, Z. H., Vincent, F., Zhang, M., Smith, N. L., Turkenburg, J. P., Charnock, S. J., Black, G. W. & Taylor, E. J. (2011). *Proteins*, **79**, 965–974.
Emsley, P., Lohkamp, B., Scott, W. G. & Cowtan, K. (2010). *Acta Cryst.* D**66**, 486–501.
Féthière, J., Eggimann, B. & Cygler, M. (1999). *J. Mol. Biol.* **288**, 635–647.
Garron, M. L. & Cygler, M. (2010). *Glycobiology*, **20**, 1547–1573.
Gerstein, M. & Krebs, W. (1998). *Nucleic Acids Res.* **26**, 4280–4290.
Gimmestad, M., Sletta, H., Ertesvåg, H., Bakkevig, K., Jain, S., Suh, S., Skjåk-Braek, G., Ellingsen, T. E., Ohman, D. E. & Valla, S. (2003). *J. Bacteriol.* **185**, 3515–3523.
Hooft, R. W., Vriend, G., Sander, C. & Abola, E. E. (1996). *Nature (London)*, **381**, 272.
Huang, W., Boju, L., Tkalec, L., Su, H., Yang, H.-O., Gunay, N. S., Linhardt, R. J., Kim, Y. S., Matte, A. & Cygler, M. (2001). *Biochemistry*, **40**, 2359–2372.
Hubbard, S. J. & Thornton, J. M. (1993). *NACCESS*. Department of Biochemistry and Molecular Biology, University College, London.
Jedrzejas, M. J., Mello, L. V., de Groot, B. L. & Li, S. (2002). *J. Biol. Chem.* **277**, 28287–28297.
Laskowski, R. A., MacArthur, M. W., Moss, D. S. & Thornton, J. M. (1993). *J. Appl. Cryst.* **26**, 283–291.
Li, S. & Jedrzejas, M. J. (2001). *J. Biol. Chem.* **276**, 41407–41416.
Li, S., Taylor, K. B., Kelly, S. J. & Jedrzejas, M. J. (2001). *J. Biol. Chem.* **276**, 15125–15130.
Lombard, V., Bernard, T., Rancurel, C., Brumer, H., Coutinho, P. M. & Henrissat, B. (2010). *Biochem J.* **432**, 437–444.
Lunin, V. V., Li, Y., Linhardt, R. J., Miyazono, H., Kyogashima, M., Kaneko, T., Bell, A. W. & Cygler, M. (2004). *J. Mol. Biol.* **337**, 367–386.
Luzzati, V. (1952). *Acta Cryst.* **5**, 802–810.
Maruyama, Y., Hashimoto, W., Mikami, B. & Murata, K. (2005). *J. Mol. Biol.* **350**, 974–986.
Maruyama, Y., Mikami, B., Hashimoto, W. & Murata, K. (2007). *Biochemistry*, **46**, 781–791.
Mello, L. V., De Groot, B. L., Li, S. & Jedrzejas, M. J. (2002). *J. Biol. Chem.* **277**, 36678–36688.
Murata, K., Inose, T., Hisano, T., Abe, S., Yonemoto, Y., Yamashita, T., Takagi, M., Sakaguchi, K., Kimura, A. & Imanaka, T. (1993). *J. Ferment. Bioeng.* **76**, 427–437.
Noble, M. E. M., Zeelen, J. P. & Wierenga, R. K. (1993). *Proteins*, **16**, 311–326.
Nukui, M., Taylor, K. B., McPherson, D. T., Shigenaga, M. K. & Jedrzejas, M. J. (2003). *J. Biol. Chem.* **278**, 3079–3088.
Ochiai, A., Yamasaki, M., Mikami, B., Hashimoto, W. & Murata, K. (2010). *J. Biol. Chem.* **285**, 24519–24528.
Ogura, K., Yamasaki, M., Mikami, B., Hashimoto, W. & Murata, K. (2008). *J. Mol. Biol.* **380**, 373–385.
Osawa, T., Matsubara, Y., Muramatsu, T., Kimura, M. & Kakuta, Y. (2005). *J. Mol. Biol.* **345**, 1111–1118.

Otwinowski, Z. & Minor, W. (1997). *Methods Enzymol.* **276**, 307–326.
Peciña, A., Pascual, A. & Paneque, A. (1999). *J. Bacteriol.* **181**, 1409–1414.
Ponnuraj, K. & Jedrzejas, M. J. (2000). *J. Mol. Biol.* **299**, 885–895.
Preston, L. A., Wong, T. Y., Bender, C. L. & Schiller, N. L. (2000). *J. Bacteriol.* **182**, 6268–6271.
Ramachandran, G. N. & Sasisekharan, V. (1968). *Adv. Protein Chem.* **23**, 283–438.
Rigden, D. J., Botzki, A., Nukui, M., Mewbourne, R. B., Lamani, E., Braun, S., von Angerer, E., Bernhardt, G., Dove, S., Buschauer, A. & Jedrzejas, M. J. (2006). *Glycobiology*, **16**, 757–765.
Rigden, D. J. & Jedrzejas, M. J. (2003). *J. Biol. Chem.* **278**, 50596–50606.
Shaya, D., Zhao, W., Garron, M. L., Xiao, Z., Cui, Q., Zhang, Z., Sulea, T., Linhardt, R. J. & Cygler, M. (2010). *J. Biol. Chem.* **285**, 20051–20061.
Skrzypczak-Jankun, E., Borbulevych, O. Y., Zavodszky, M. I., Baranski, M. R., Padmanabhan, K., Petricek, V. & Jankun, J. (2006). *Acta Cryst.* D**62**, 766–775.
Spek, A. L. (2003). *J. Appl. Cryst.* **36**, 7–13.
Thompson, J. D., Higgins, D. G. & Gibson, T. J. (1994). *Nucleic Acids Res.* **22**, 4673–4680.
Tsitsanou, K. E., Oikonomakos, N. G., Zographos, S. E., Skamnaki, V. T., Gregoriou, M., Watson, K. A., Johnson, L. N. & Fleet, G. W. (1999). *Protein Sci.* **8**, 741–749.
Winn, M. D. *et al.* (2011). *Acta Cryst.* D**67**, 235–242.
Yamasaki, M., Ogura, K., Hashimoto, W., Mikami, B. & Murata, K. (2005). *J. Mol. Biol.* **352**, 11–21.
Yonemoto, Y., Tanaka, H., Hisano, T., Sakaguchi, K., Abe, S., Yamashita, T., Kimura, A. & Murata, K. (1993). *J. Ferment. Bioeng.* **75**, 336–342.
Yoon, H.-J., Hashimoto, W., Miyake, O., Murata, K. & Mikami, B. (2001). *J. Mol. Biol.* **307**, 9–16.
Yoon, H.-J., Hashimoto, W., Miyake, O., Okamoto, M., Mikami, B. & Murata, K. (2000). *Protein Expr. Purif.* **19**, 84–90.
Yoon, H.-J., Mikami, B., Hashimoto, W. & Murata, K. (1999). *J. Mol. Biol.* **290**, 505–514.